ISSN 1063-7729, Astronomy Reports, 2008, Vol. 52, No. 3, pp. 211–225. © Pleiades Publishing, Ltd., 2008.
Original Russian Text © M.I. Pashchenko, A.M. Tolmachev, E.E. Lekht, 2008, published in Astronomicheskiĭ Zhurnal, 2008, Vol. 85, No. 3, pp. 241–256.

Maser Emission Toward the Very Young Massive Star GH_2O 092.67+03.07 (IRAS 21078+5211)

M. I. Pashchenko[1], A. M. Tolmachev[2], and E. E. Lekht[3]

[1] *Sternberg Astronomical Institute, Universitetskiĭ prospekt 13, Moscow, 119991 Russia*

[2] *Pushchino Radio Astronomy Observatory, Astrospace Center of the Lebedev Institute of Physics, Russian Academy of Sciences, Pushchino, Moscow oblast', 142290 Russia*

[3] *Instituto Nacional de Astrofísica, Óptica y Electrónica, Luis Enrique Erro No. 1, Apdo Postal 51 y 216, 72840 Tonantzintla, Puebla, México*

Received June 17, 2007; in final form, June 22, 2007

Abstract—Results of monitoring of the H_2O maser observed toward the infrared source IRAS 21078+5211 in the giant molecular cloud Cygnus OB7 are presented. The observations were carried out on the 22-m radio telescope of the Pushchino Radio Astronomy Observatory (Russia) from April 1992 to March 2006. Five cycles of maser activity at various levels were observed. In the periods of highest activity, the spectrum of the H_2O maser emission extended from −43 to 12 km/s. During strong flares, the flux densities in some emission features reached nearly 600 Jy. The protostar has a small peculiar velocity with respect to the CO molecular cloud (∼2 km/s). Based on the character of the radial-velocity variations and the tendency for the linewidth to increase with the flux, it is concluded that the medium is strongly fragmented and that there is a small-scale turbulent outflow of gas in the H_2O maser region, which may impede the formation of an HII region. The asymmetric distribution of the maser components in V_{LSR}, the difference in the average linewidths of the central and lateral clusters of components, and the fairly high radial velocities relative to the molecular cloud (especially during periods of the highest maser activity) suggest that the maser spots belong to different clusters and different structures of the source: a disk and bipolar outflow.

PACS numbers: 97.10.Fy, 95.85.Bh
DOI: 10.1134/S1063772908030049

1. INTRODUCTION

At an early stage of their formation, stars are embedded in dense, cold gas–dust clouds, in which the protostar is not visible in the optical due to the very large extinction. Its emission is absorbed in the protostellar cloud and then re-radiated in the far infrared. At an early stage of their evolution, stars pass through a stage with a very energetic outflow of material accompanied by the formation of powerful high-velocity bipolar (sometimes unipolar) outflows of cold molecular gas. H_2O masers, then OH and methanol masers, appear in the vicinity of the star (in a cloud surrounding the star) in this stage, and an ultracompact HII region is formed. Water masers can be associated either with a disk around the protostar or with high-velocity bipolar molecular outflows.

Water maser emission at $\lambda = 1.35$ cm was detected toward IRAS 21078+5211 in January 1989 [1]. The maser spectrum had three peaks at −27, −17.6, and −14 km/s with flux densities of 15, 41, and 23 Jy, respectively. Water maser emission had actually been observed even earlier (July 27, 1988), but these results were published only in 1993 [2]. The main peak with a flux density of 3.7 Jy had a velocity of −21.4 km/s. In May 1991, no emission was detected. The subsequent interferometric measurements of Jenness et al. [3] showed that the H_2O maser is located more than 1′ south of the IR source (IRAS 21078+5211) and an associated HII region. The maser is not related to the IR source, and instead exactly coincides with the position of a source of submillimeter radiation. Consequently, there appear to be two independent sources within the same extended and massive (more than 900 $M_\odot$) dust envelope.

Thus, the H_2O maser is located in the Cygnus OB7 giant molecular cloud 800 pc from the Sun [4]. High-mass stars are being formed in this region. The total mass of the dense gas cloud is $7.7 \times 10^4\ M_\odot$. The H_2O maser is associated with a young massive star called GH_2O 092.67+03.07. The exact coordinates of the maser and protostar

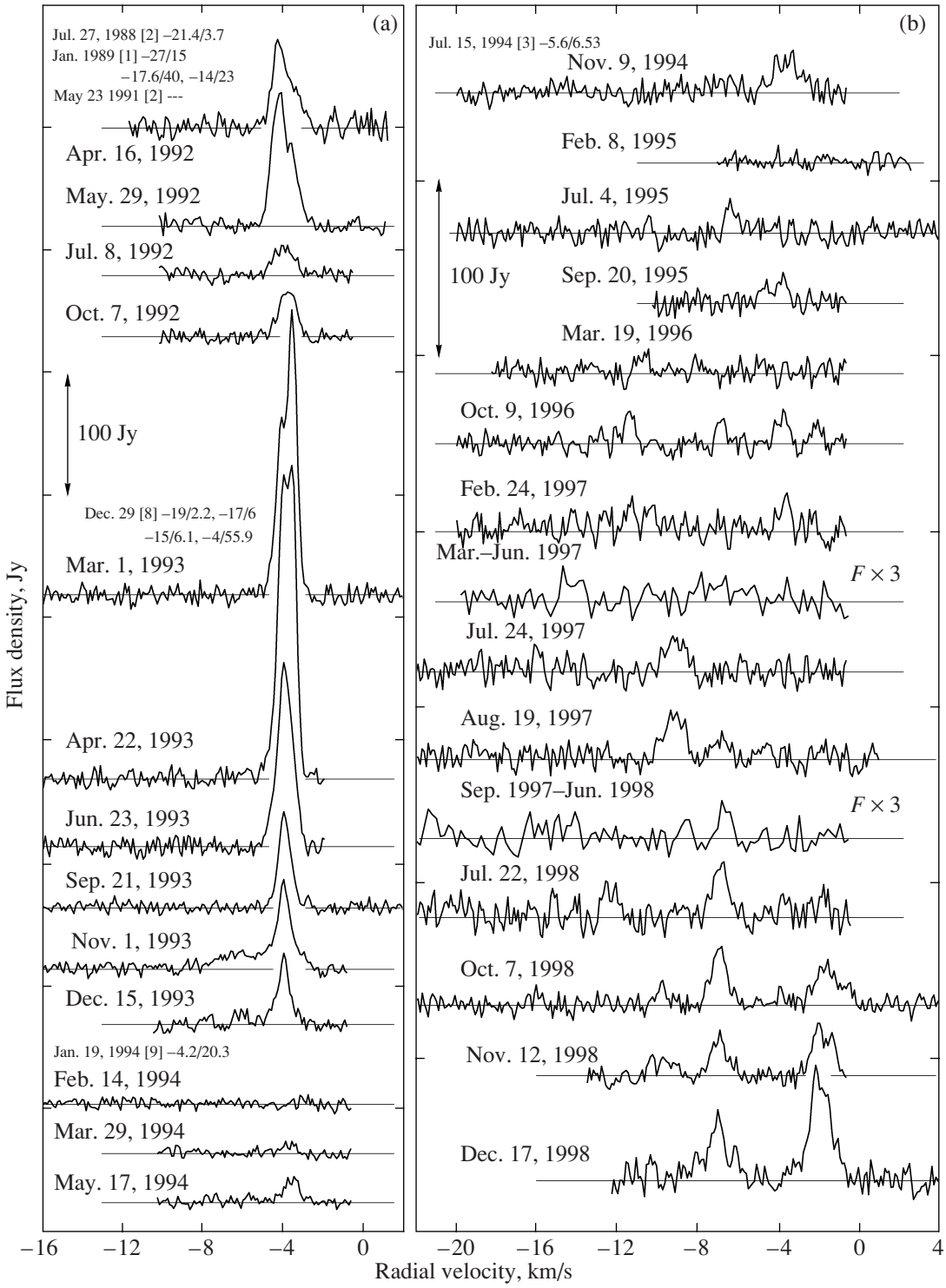

Fig. 1. Catalog of spectra of the H_2O maser emission toward IRAS 21078+5211. The double-pointed arrow shows the scale. The radial velocities are relative to the Local Standard of Rest. The observational data of other authors (date, reference, and velocity/flux for various emission peaks) are shown in smaller font.

are $\alpha_{1950} = 21^{\rm h}07^{\rm m}46.65^{\rm s}$, $\delta_{1950} = 52^\circ10'22.8''$ ($l = 92.67^\circ$, $b = +3.07^\circ$).

Bernard et al. [5] interpreted millimeter and submillimeter interferometric observations using a model with a dense, contracting, rotating disk with a very young bipolar outflow emanating from its center. They estimate the dynamical timescale of the outflow to be $\simeq 3.5 \times 10^3$ years, and its linear size to be

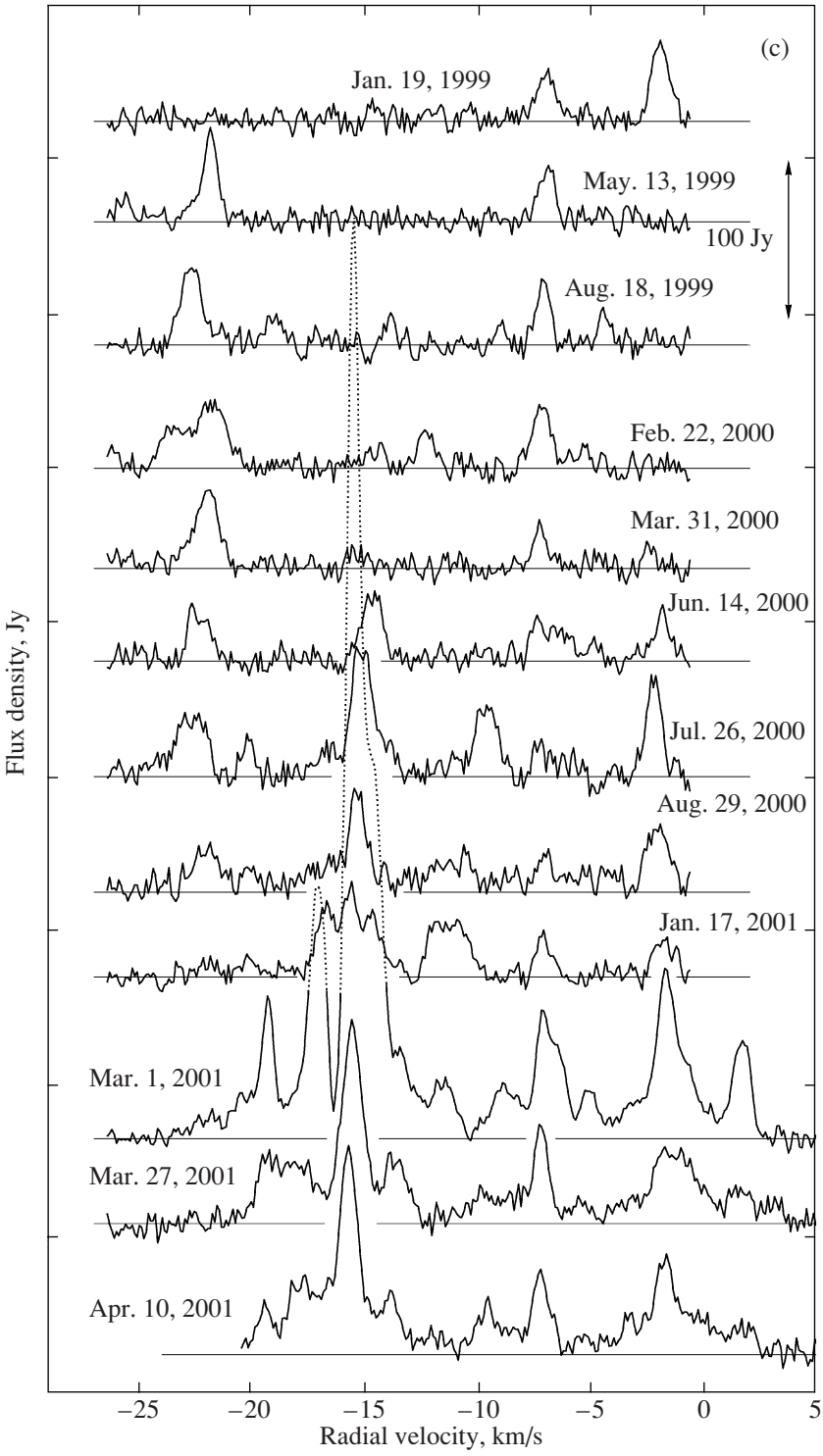

Fig. 1 (Contd.)

8×10^3 AU. The masses of the outflow and disk are 0.6 and 12 $M_\odot$, respectively.

The disk center hosts a protostar with a mass of 4.1–7.4 $M_\odot$ [5]. Szymczak et al. [6] detected no hydroxyl or methanol maser emission toward this protostar. No radio continuum emission was detected at 8 GHz, $F < 0.3$ mJy; i.e., no HII region was detected. All this suggests that the massive star is rather young.

The velocities of molecular lines observed toward IRAS 21078+5211 are $V_{\rm LSR}({\rm CS}) = -6.2$ km/s [5]

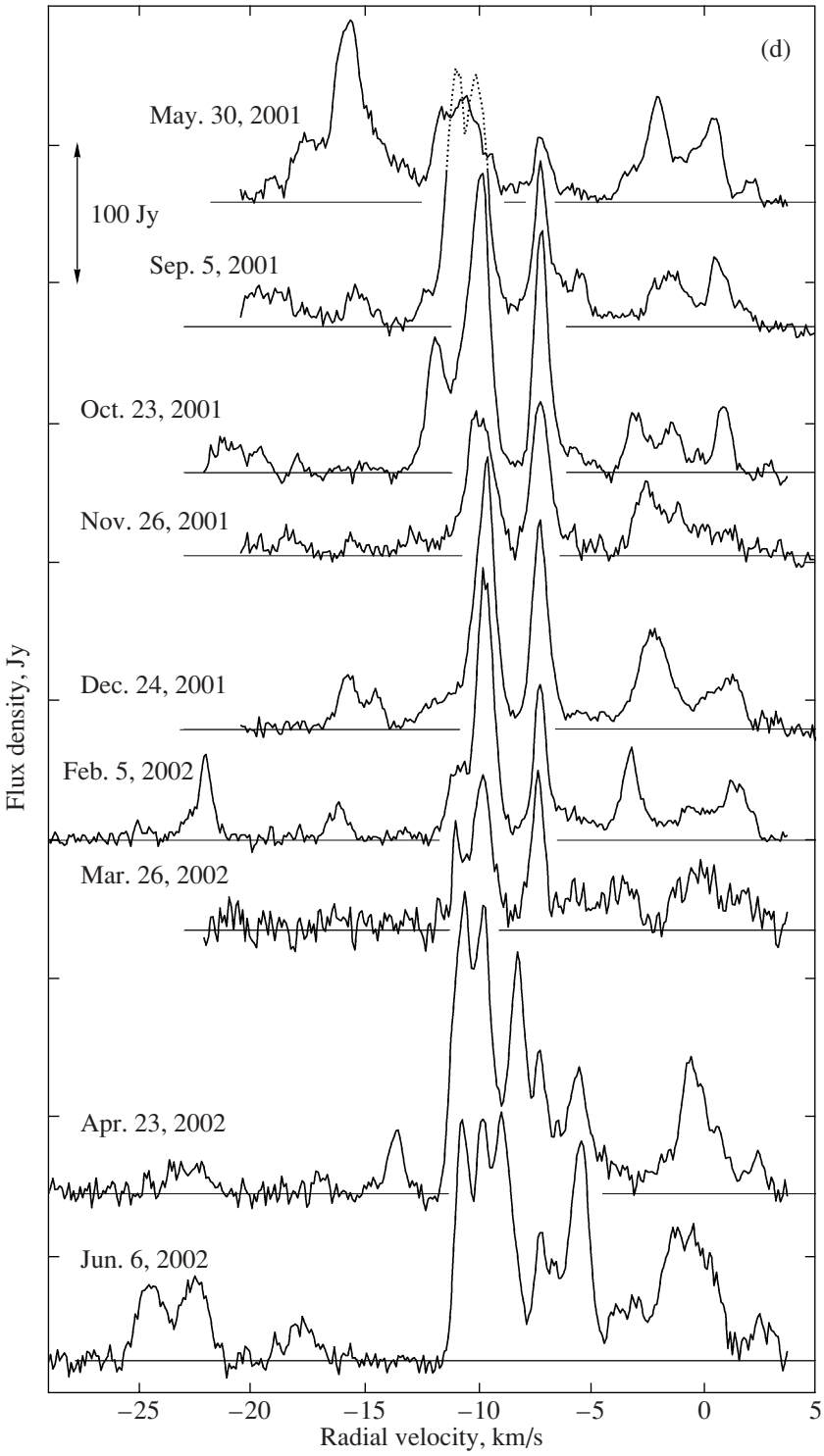

Fig. 1 (Contd.)

and −6.8 km/s [3], $V_{\rm LSR}({\rm CO}) = -6.1$ km/s [7], $V_{\rm LSR}(^{12}{\rm CO}) = -6.9$ km/s [5] and −5.5 km/s [3]. The velocities of ammonia lines are −6.5 km/s ($J = 1$, $K = 1$) and −6.3 km/s ($J = 2$, $K = 2$), with their linewidths being 1.64 and 2.49 km/s, respectively [8]. The presence of warm ammonia (∼20 K) confirms the relation of the molecular gas to the embedded maser source.

Our current study is concerned with the results of monitoring of the H_2O maser at 1.35 cm in IRAS 21078+5211 during 1992–2006.

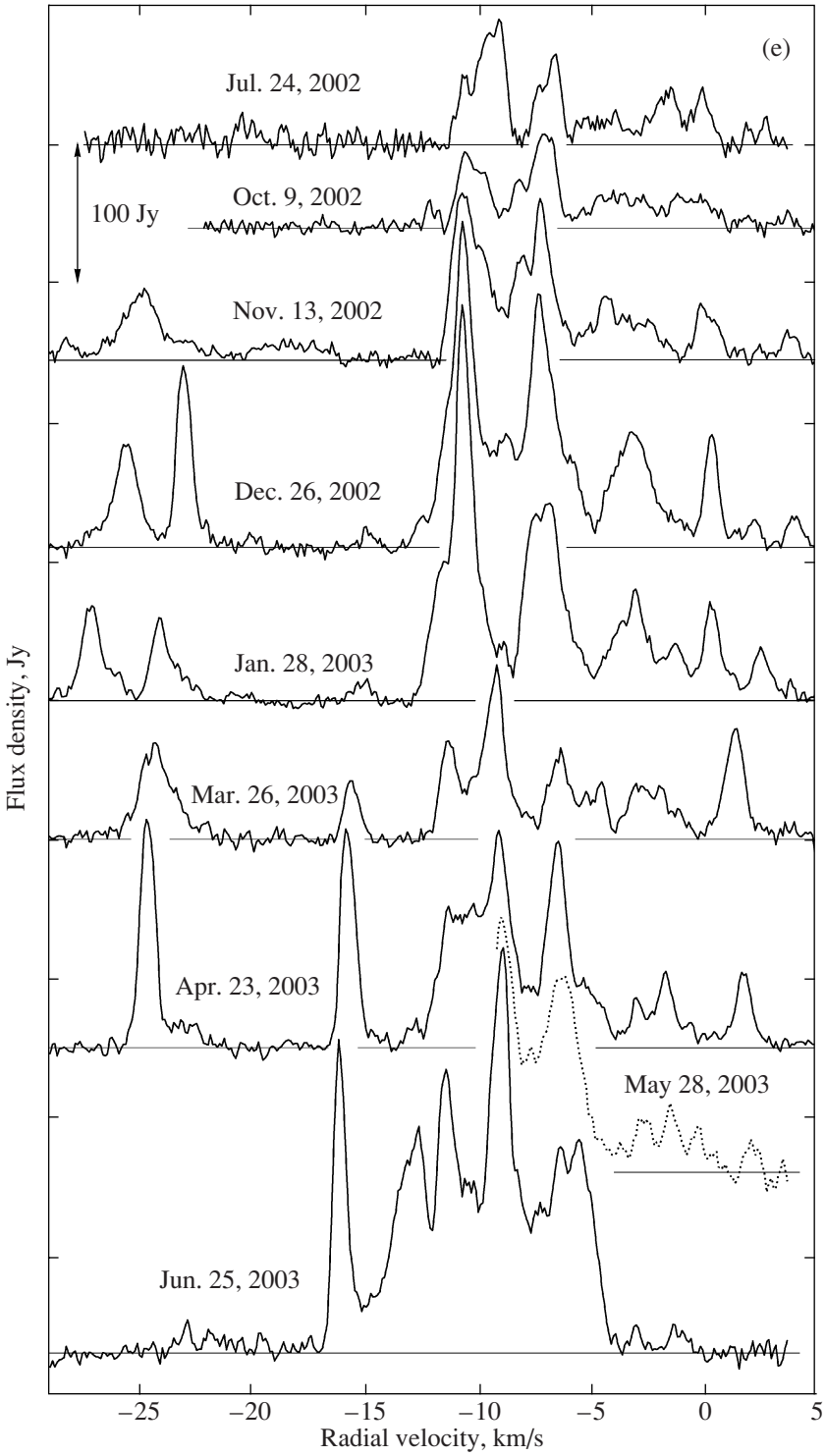

Fig. 1 (Contd.)

2. OBSERVATIONS AND DATA REDUCTION

Our observations of H_2O maser emission toward IRAS 21078+5211 were carried out on the 22-m radio telescope of the Pushchino Radio Astronomy Observatory from April 1992 to March 2006. The mean interval between observations was two months. The noise temperature of the system with a cooled FET amplifier at the frontend was 150–230 K. A

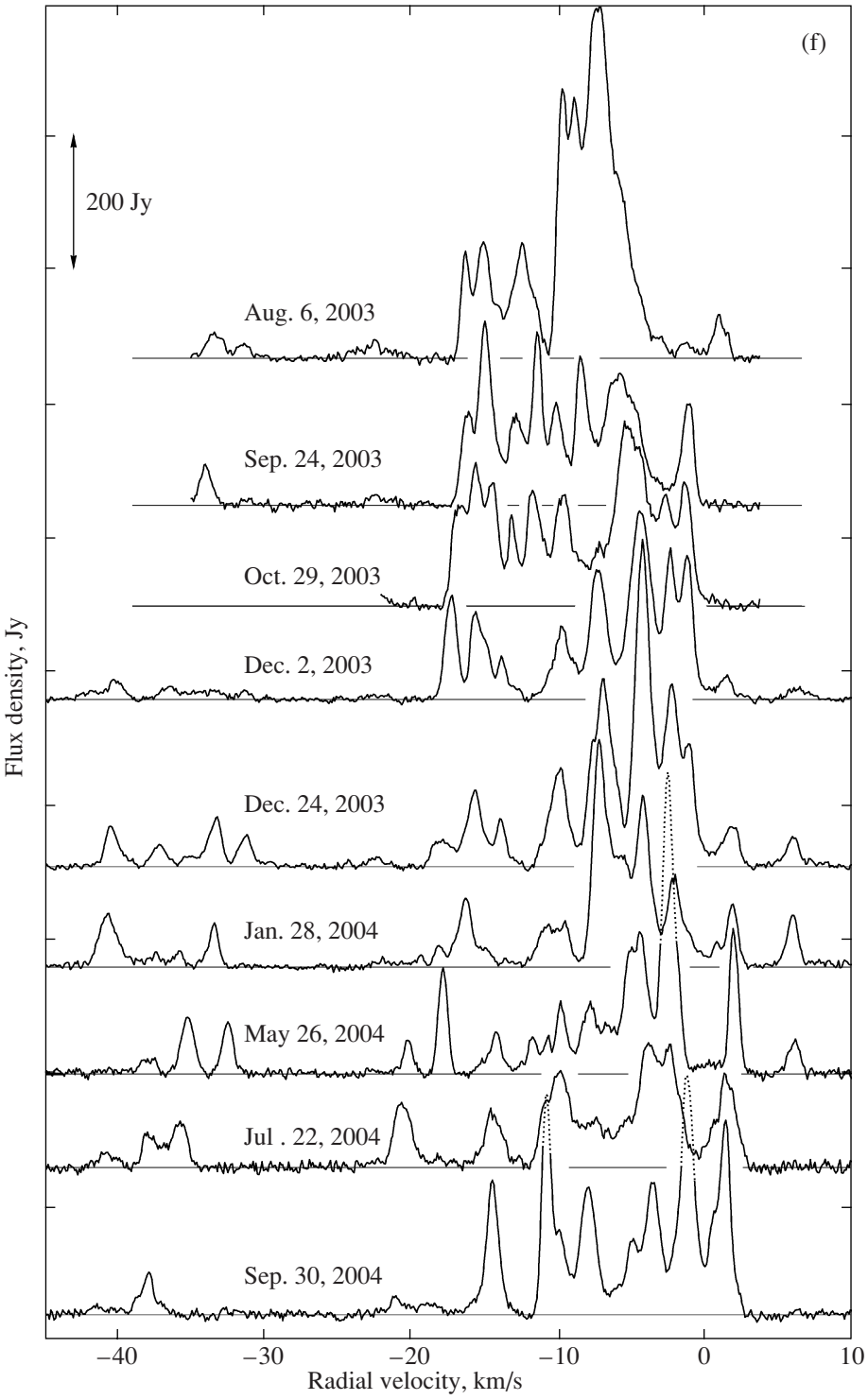

Fig. 1 (Contd.)

radiometer upgrade in 2000 lowered the system noise temperature to 100–130 K.

The signals were analyzed using a 96-channel (starting in July 1997, 128-channel) filter-bank spectrum analyzer with a resolution of 7.5 kHz (0.101 km/s in radial velocity in the 1.35-cm line). Starting at the end of 2005, a 2048-channel autocorrelator with a resolution of 6 kHz (0.0808 km/s at 22 GHz) was used. For pointlike source, an antenna

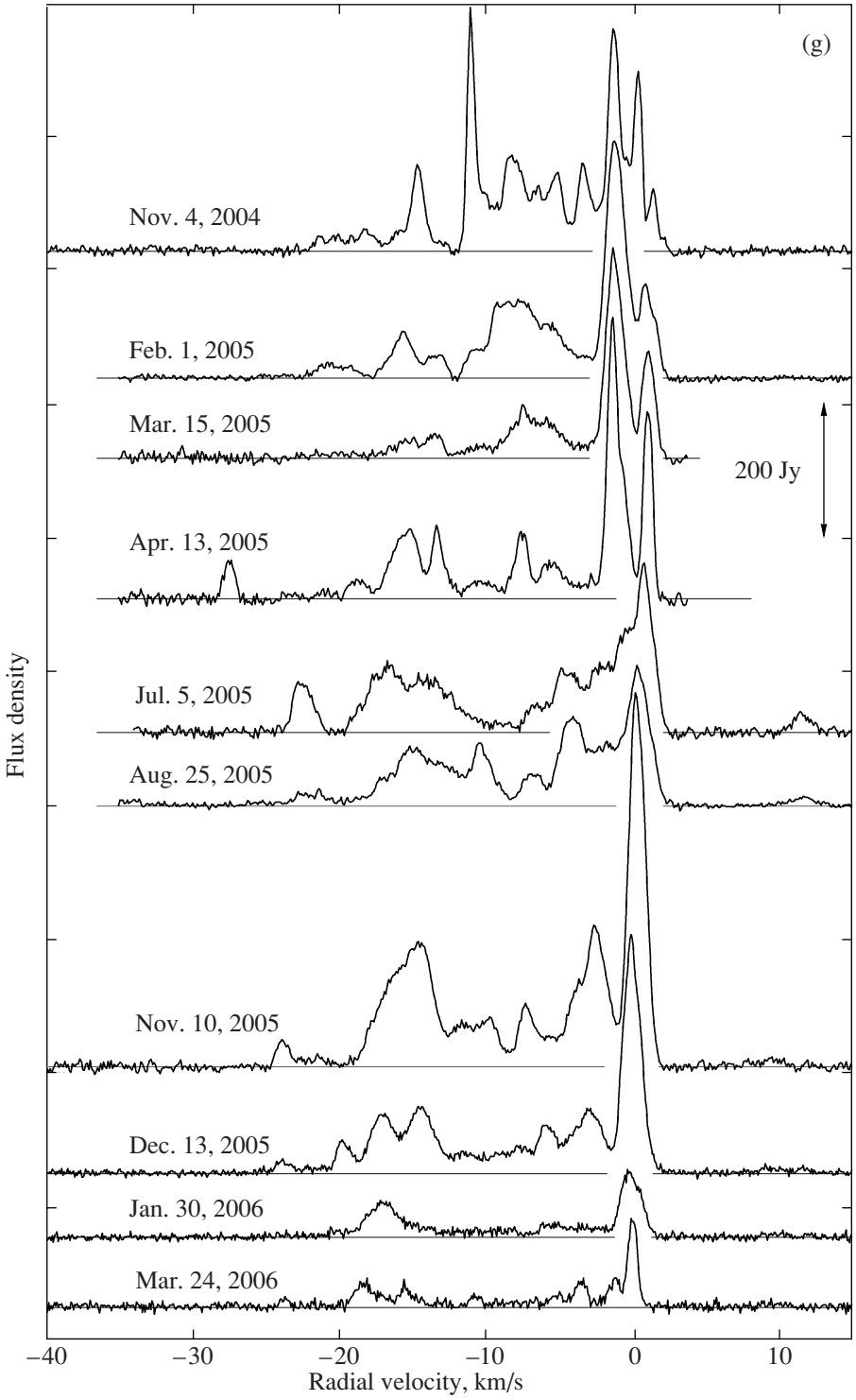

Fig. 1 (Contd.)

temperature of 1 K corresponds to a flux density of 25 Jy.

Figure 1 presents a catalog of the H_2O spectra. The double-pointed arrow shows the scale in Janskys. The horizontal axis plots the velocity relative to the Local Standard of Rest. For convenience, zero baselines are drawn in each spectrum.

The figures with spectra for April 1992 to June 2003 are shown on identical scales on both axes, except for Fig. 1b, where the flux scale has been expanded in view of the weaker signal. Beginning in

the second half of 2003, the maser activity strongly increased and the emission velocity range broadened; we changed the scales on both axes accordingly. The smaller font in Figs. 1a and 1b shows data obtained by other authors in chronological order. The dates of observations (day, month, and year), reference (in square brackets), and the velocity/flux ratio for various emission peaks are indicated.

Since the signal was not visible in individual spectra obtained from March to June 1997 and from September 1997 to June 1998, we averaged the spectra for these intervals, and also averaged in each spectrum pairs of adjacent channels at the expense of a twofold reduction in the spectral resolution. The flux scale for these averaged spectra, labeled (03–06).1997 and 09.1997–06.1998 in Fig. 1b, has been expanded threefold.

Figure 2 plots a superposition of all the H_2O spectra for which emission was detected for three different time intervals. The spectrum can be divided into three segments: the central (main) region and two lateral region. The boundaries are determined by the emission minimum, which lie near radial velocities of −21 and +2.5 km/s. The division of the main body of the spectrum into segments (where individual emission features are clustered) is outlined for the first two intervals (Figs. 2a and 2b); such a division is obviously absent starting from the end of 2002.

Figures 3a and 3b show the variability of the integrated flux $F_{\rm int}$ and velocity centroid $V_{\rm c}$ (weighted-mean radial velocity), respectively. Both parameters of the H_2O maser emission were calculated for radial velocities from ≈−21 to ≈2.5 km/s. The small uncertainty in delimiting the spectra was ±0.5 km/s, and was due to the presence of weak emission near the boundaries of the spectrum segment. According to the $F_{\rm int}$ variability, the 14-year monitoring interval can be divided into cycles of activity of the H_2O maser emission with durations of 2.5–3 yrs each. The boundaries of the cycles are shown by vertical dashed lines. We have approximated the variability of $V_{\rm c}$ by a smoothed curve (dashed curve in Fig. 3b). The dotted lines show the tendency for $F_{\rm int}$ to increase in cycle *3* and the average value of this quantity for cycles *4* and *5*.

The vertical lines show the radial-velocity intervals in which H_2O maser emission was observed for each spectral segment (Fig. 3c). Note that the radial-velocity range in which maser emission was observed expanded with enhancement of the maser activity. This could be due to differences in the physical parameters of the medium hosting the maser spots; we cannot rule out the possibility that they belong to different structures in the source, such as a disk and bipolar outflow.

The H_2O spectra contain a large number (more than 20) individual emission features, especially during periods of high maser activity. We attempted to distinguish these spectral components by fitting them with Gaussians. The difficulty was that, in some regions of the spectrum, components with nearby radial velocities sometimes overlapped. In these cases, fitting Gaussians was not useful due, for example, to the large errors in the resulting linewidths. In such cases, we determined only two parameters for the emission: its radial velocity and flux. Despite these limitations, the completeness of our analysis of the monitoring data was more than 90%.

Figure 4 shows the time dependence of the radial velocities for isolated components at velocities from −45 to +15 km/s. The filled circles show components for which three parameters (flux, radial velocity, and linewidth) were determined, and the open circles those for which the linewidth could not be determined with sufficient confidence.

The emission variability turned out to be fairly strong, and some components were observed over one to two years, while the rest lived for shorter times. The emission drifted in radial velocity. In most cases, the variations in the emission peak velocities were probably random (see insert in Fig. 4). One possible origin of such variations could be strong fragmentation in the medium hosting the maser spots, as well as the presence of small-scale turbulent motions on scales comparable to the maser spot sizes. The spot sizes for sources at a very early stage of their evolution are usually of the order of 0.1 AU (see, e.g., [9]). For this reason, we have included in our statistical database all components detected in all our monitoring spectra as independent events. The total number of components (events) is 684. This enabled us to also find some characteristics for determining a possible model for the H_2O maser; e.g., the most probable velocities of the maser emission.

Figure 5 (left) shows the dependences between the linewidths (δV) and radial velocities ($V_{\rm LSR}$) and (right) between δV and the fluxes (F_ν) for the five cycles of maser activity (Figs. 5a–5e) and the entire monitoring interval (Fig. 5f). The boundaries of the activity cycles are indicated in the left-hand plots. In Fig. 5f, the two solid lines forming a cone mark the most preferential locations of the components. The dashed lines outline two small sequences of points that simply drop out of the cone space, and are in no way linked to each other by evolutionary factors.

A division of the components into radial-velocity groups is observed in the activity cycles; we have labeled these groups A, B, and C. The mean linewidths for each group are given in parentheses. In cycle *4* (Fig. 5d), the division into groups A and B is drawn at $V_{\rm LSR} = -17.5$ km/s.

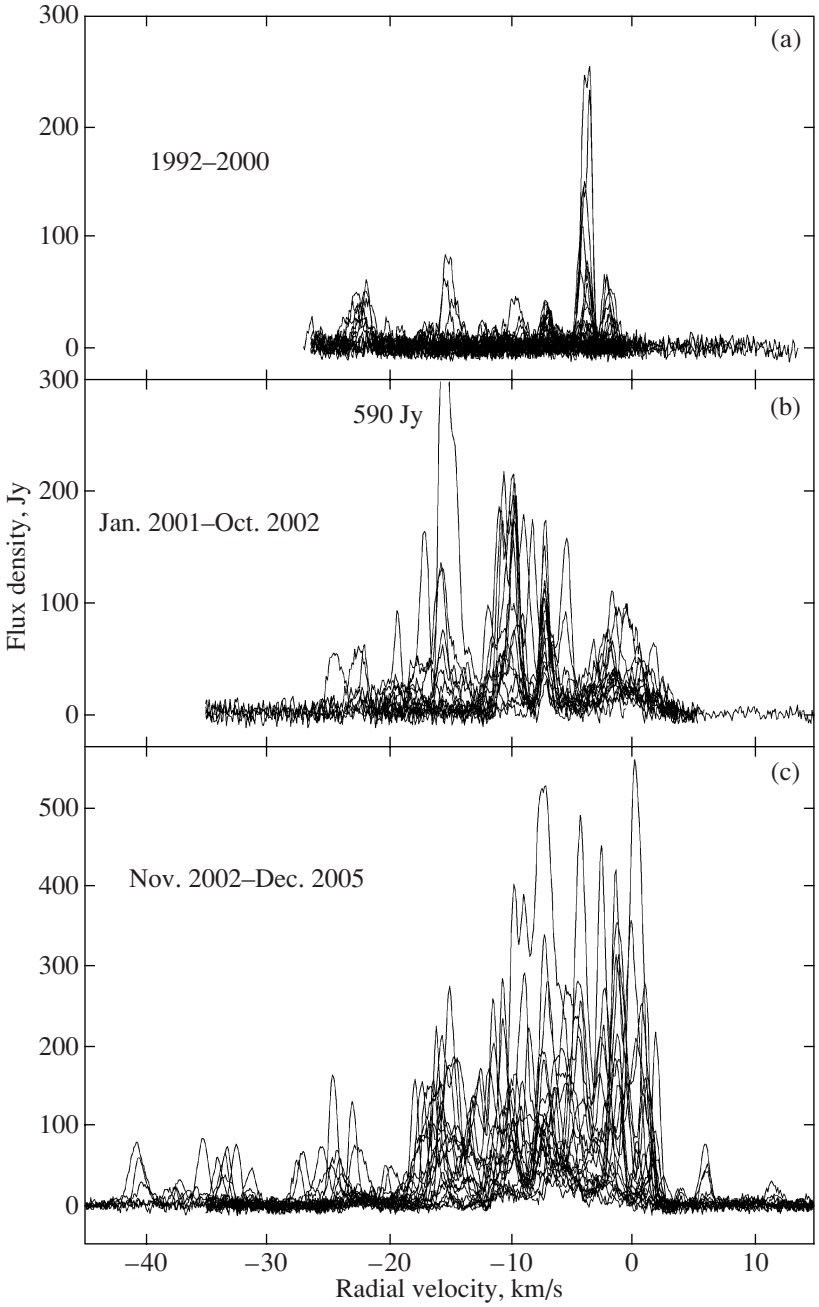

Fig. 2. Superposition of the H_2O spectra for various time intervals.

Using the same statistical database, we have plotted three histograms of the distributions of the number of components N (which we call events) in V_{LSR}, δV, and F_ν (Fig. 6). In the top graph, we have approximated the histogram by a smooth curve to which Gaussians have been fitted, with the positions of their maxima indicated.

In the middle graph, we have fitted a Gaussian with a peak at 0.74 km/s; this is the most typical linewidth for a single component in the H_2O maser emission associated with IRAS 21078+5211. The distribution in the bottom graph was approximated by an exponent. A histogram on a logarithmic scale is shown to the right. The lack of a number of the components at the very beginning of the distribution ($F_\nu < 20$ Jy) could be due to the limited sensitivity, and hence to some selection effects. We have also included in the histograms of Fig. 6a components for which we could not determine accurate linewidths.

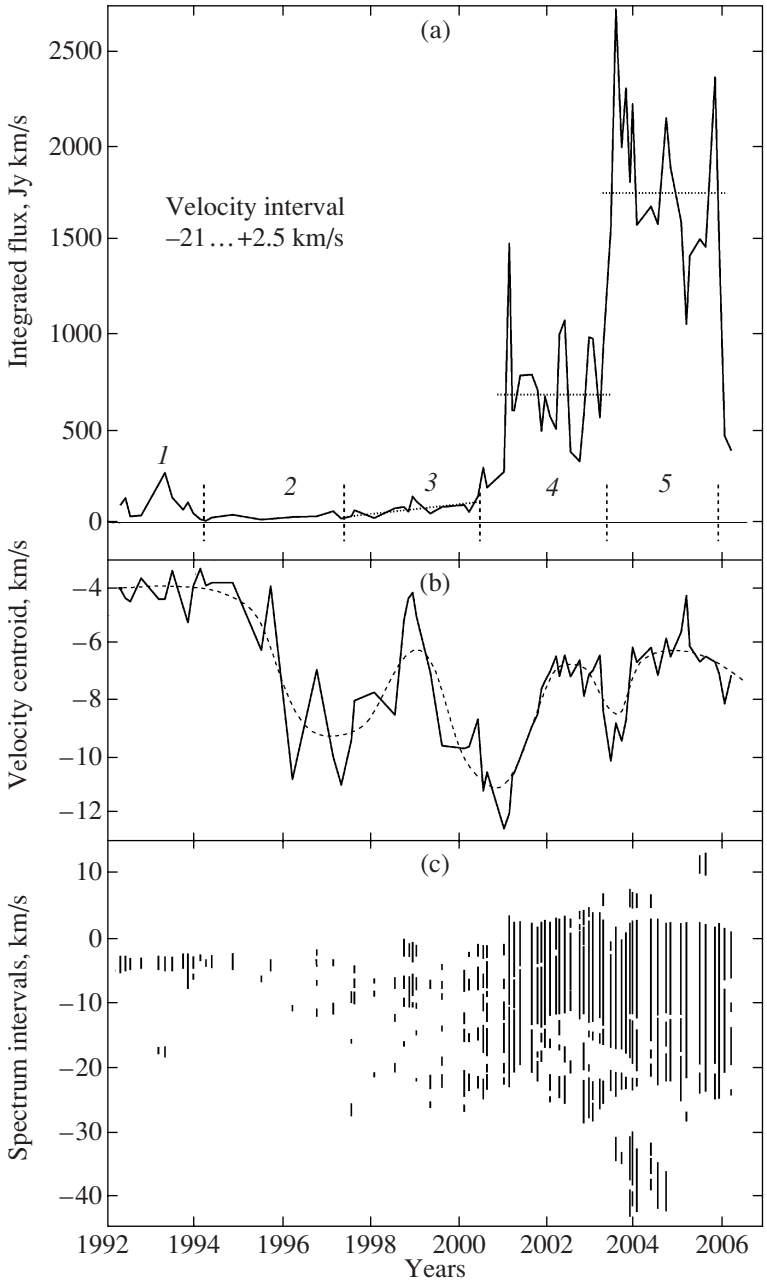

Fig. 3. (a) Variations of the integrated flux at radial velocities from ∼−21 to ∼2.5 km/s; (b) variations of the velocity centroid for the same interval; (c) velocity intervals of the H_2O spectra in which maser emission was observed. The vertical dashed lines in the upper panel divide the full monitoring interval into individual cycles of maser activity (*1*–*5*). The dotted lines show the tendency for $F_{\rm int}$ to grow in cycle *3* and its average value for cycles *4* and *5*. The variations of the velocity centroid (middle panel) are approximated with a smoothed curve (dashed).

3. DISCUSSION

Due to the long duration of our monitoring of the maser emission in IRAS 21078+5211 (14 years), we were able to observe the source in quite different stages of its activity: from a full absence of maser emission to a state when the spectrum contained a large number of emission features with flux densities of 300–600 Jy. In the latter case, the velocity range expanded to 55 km/s, extending from $V_{\rm min} = -43$ km/s to $V_{\rm max} = 12$ km/s.

3.1. Activity Cycles of the H_2O Maser Emission

For convenience in our analysis of the maser emission, we have introduced five cycles of activity of the maser source (Fig. 3a). Let us consider the first of these.

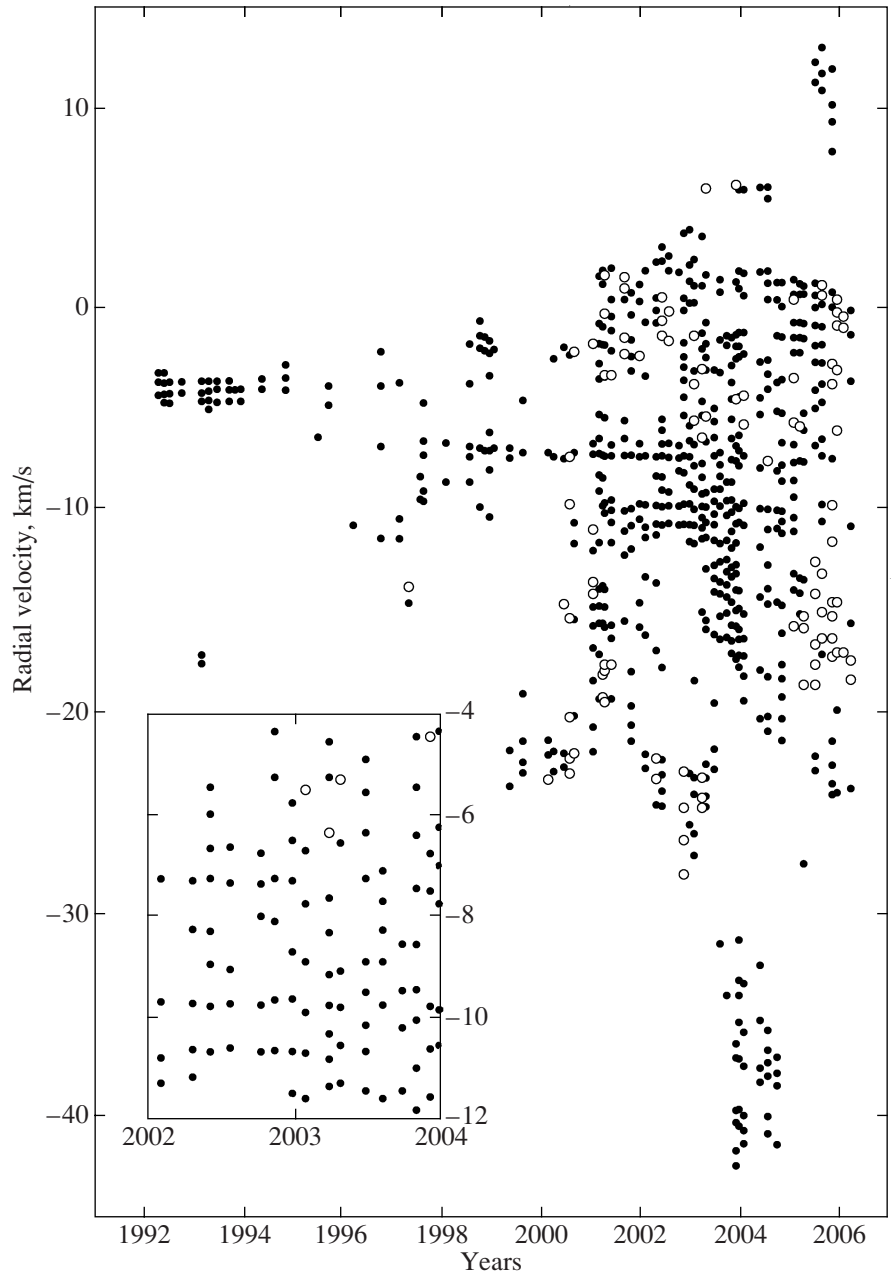

Fig. 4. Radial-velocity variations of individual emission features in the V_{LSR} interval from −45 to +15 km/s. The filled circles show components for which the flux, radial velocity, and linewidth have been measured, and the open circles components for which only the first two parameters have been determined. The insert shows a fragment on an expanded scale.

The H_2O emission was first observed in July 1988. The maser emission has been observed several times since then [1–3, 10], but these were epochs of fairly low activity. In 1989, the emission flux of one of the peaks reached 40 Jy. Interferometric measurements of the maser emission was carried out when the peak flux was only 6.5 Jy. At all these epochs, the extent of the spectrum was 15–25 km/s and the maser emission tended to be shifted toward higher velocities. In particular, the velocity centroids in July 1988 and January 1989 were −17.9 and −19.8 km/s, respectively. No emission was detected in May 1991, and it was observed at $V_{LSR} = -4$ km/s in 1992 (this work). This emission probably appeared in the second half of 1991, in which case this can be taken to be the beginning of the first cycle. The years 1992–1993 are characterized by a considerable increase in the maser emission to 250 Jy, with this emission appearing at radial velocities close to the velocity of the CO molecular cloud ($\sim$−6 km/s).

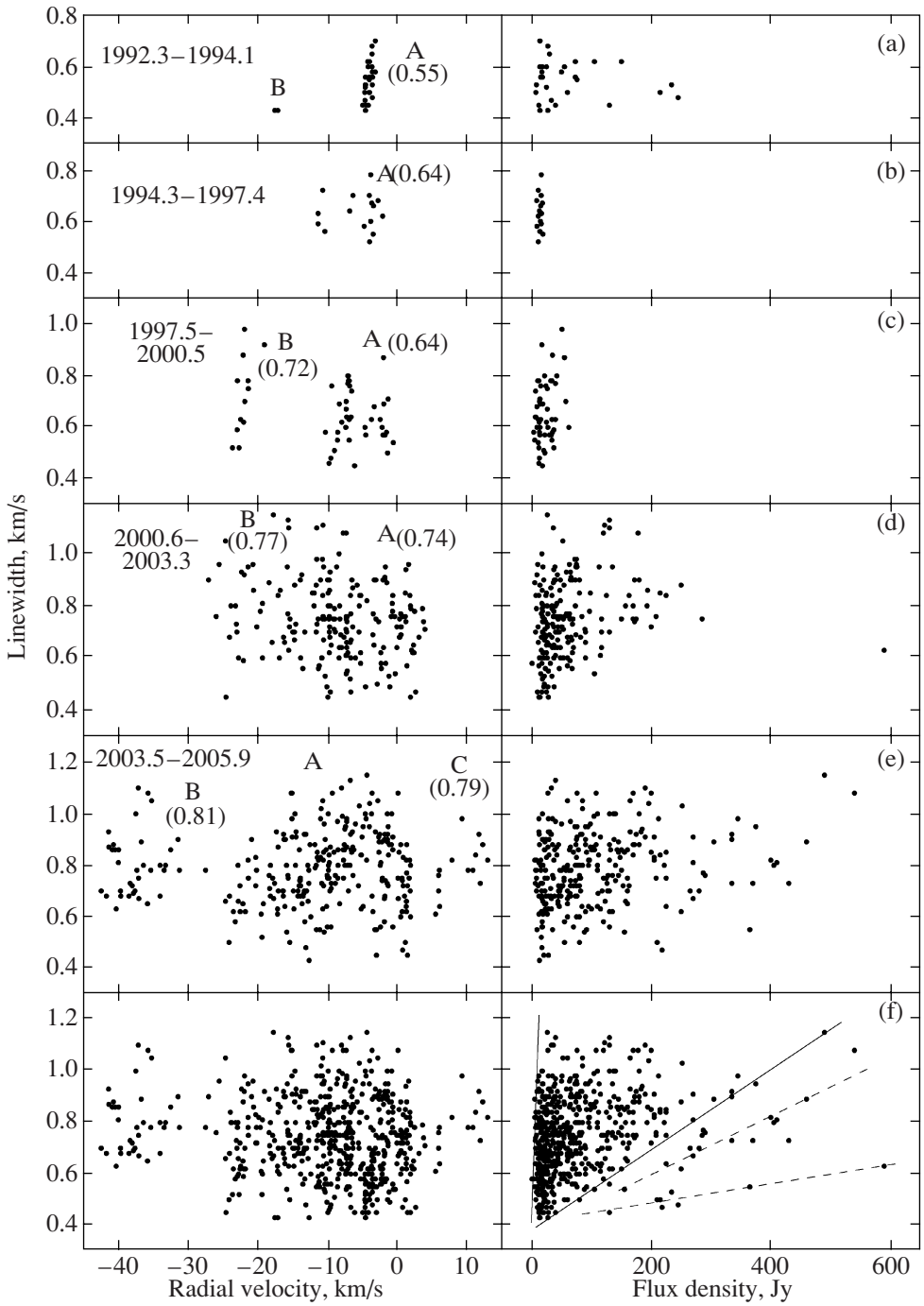

Fig. 5. Linewidths of individual components as a function of the radial velocity (left) and flux density (right) for the different cycles of maser activity (a)–(e) and for the entire monitoring interval (f). See text for details.

As we can see from Fig. 3a, cycle *2* is characterized by a low level of H_2O maser activity. The average integrated flux was 33 Jy km/s.

In spite of the presence of strong variations of the emission, the maser activity in May 1997–May 2000 (cycle *3*) clearly displayed an increase from $F_{\rm int} = 29$ Jy km/s to $F_{\rm int} = 110$ Jy km/s (dotted line in Fig. 3a).

Beginning in mid-2000, the maser emission began to grow sharply to a mean level 700 Jy·km/s. Over the next 2.3 years (cycle *4*), $F_{\rm int}$ fluctuated widely about this level, and the velocity centroid shifted to −7 km/s, i.e., to a value close to the molecular-cloud velocity.

Cycle *5*, which was the most active one, is, in many respects, similar to cycle *4*, but $F_{\rm int}$ fluctuated

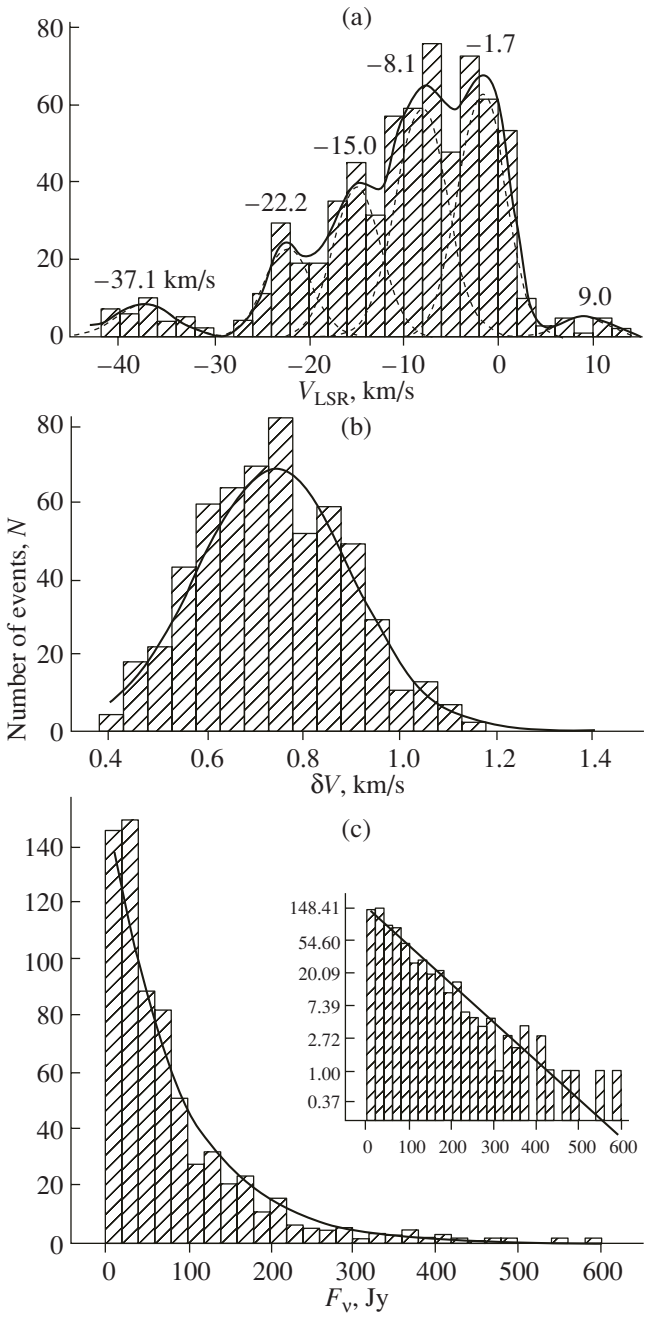

Fig. 6. Histograms of the number of events (emission features) (a) in radial velocity, (b) in linewidth, and (c) in flux. The solid curve in the top panel shows a smoothed distribution with fitted Gaussians (with the positions of their maxima). In the middle and bottom panels, a Gaussian and exponential have been fitted. A histogram in a logarithmic scale is shown to the right.

strongly about a higher level of the integrated flux and the H_2O spectra were more extended, covering up to 55 km/s (from −43 to +12 km/s). The maser emission intensity sharply dropped at the end of 2005.

An important conclusion follows from our analysis of the integrated flux variations: cycle-to-cycle transitions were fairly rapid, resembling a trigger mechanism leading to the transition from one state to another. A similar phenomenon was observed in G43.8−0.1 [11], where the duration of the cycle of highest maser activity was about 3.3 years, similar to the durations of cycles of high activity of the H_2O maser in IRAS 21078+5211. Such variations of the maser emission could be due to rapid changes in the luminosity of the protostar; thus far, this has not been observed in most other sources associated with young star-forming regions.

3.2. Individual Emission Features in the H_2O Spectrum

The decomposition of the spectra into separate components shows the presence of a large number of emission features, whose lifetimes are short. Some of these were observed over one to two years, while the rest had shorter lifetimes. In many cases, the velocities of the components varied chaotically, suggesting strong fragmentation of the medium. In addition, the variability timescale was approximately equal to the interval between observational sessions, ≈2 months.

The drift rate of the emission peaks was fairly high for components with lifetimes of about 0.5 year, reaching 1.3 km $s^{-1}yr^{-1}$. However, we observed no preferential direction for the drift, even within small radial-velocity intervals, and this direction changed somewhat chaotically from one component to another. Therefore, the observed drift cannot be due to Keplerian motion in the field of the central star, and is most likely due to the complex structure of the medium hosting the maser condensations.

The short lifetimes of the components (in their active phase) can be explained by a high rate of dissipation of the shock energy that provides the population inversion in the maser medium and an absence of a continuous"replenishment" of this energy due to a very unstable stellar wind. Certainly, the main role seems to be played by strong, fairly small-scale fragmentation of the medium.

3.3. Statistical Parameters of the Emission

Our statistical analysis has yielded a number of important results.

(1) The linewidths of the components in the lateral clusters (B and C) are larger than those in the central cluster (A) in all maser activity stages, except for the first one, when the statistics for cluster B are very poor. The average linewidths are given in parentheses in Figs. 5a–5e (to the left). This effect may be due to differences in the physical conditions where the different clusters are generated, as well as spots forming different clusters belonging to different structures within IRAS 21078+5211, e.g., a disk and bipolar outflow.

(2) The linewidth tends to increase with increasing flux (Fig. 5, right). The growth in the fluxes of emission features occurs throughout the radial-velocity interval, suggesting it was due to an enhancement of the activity of the central star and, therefore, of the pumping level. This can result in an increase in the maser spot sizes. It is known that the linewidth is determined by both thermal ans turbulent motions of molecules. It is natural to suppose that there may exist small-scale turbulence within individual maser spots.

(3) The radial-velocity distribution of the components is strongly asymmetric, ruling out models in which the masers form in a disk structure alone (see, e.g., [12]). We have fitted six Gaussians to the components. The extreme, high-velocity components could be related to bipolar outflows. It is not possible to determine the structures associated with the remaining four Gaussians. We can only point out that, at very early stages of star formation, when the HII regions just begin to be formed, maser spots are localized in gas–dust envelopes surrounding the protostar.

(4) The linewidth distribution is not completely symmetric, though it is fairly well approximated by a Gaussian with its maximum at $\delta V = 0.74$ km/s. The small asymmetry is due to the presence of clusters of components with broader lines at high velocities relative to the cloud.

(5) The distribution of the number of components in amplitude (flux) is fairly well approximated by an exponential. This result is interesting, and thus far has been obtained for this source only by us. Such a distribution could be due to properties of the medium in which the maser emission is localized. To obtain firmer conclusions, similar studies must be carried out for a number of other sources.

3.4. Model of the H_2O Maser in IRAS 21078+5211

The absence of interferometric measurements with high angular resolution prevents us from deriving an unambiguous model for the maser source.

According to Bernard et al. [5], the gas density in the disk is more than an order of magnitude higher than in the bipolar outflow. Therefore, conditions in the disk are more favorable for maser emission than those in the outflow. For this reason, only in periods of a very high activity of the protostar can conditions be favorable for maser emission in the outflow, as is confirmed by our monitoring. However, the main maser is most likely intrinsically associated precisely with the disk.

Let us return to the histogram in Fig. 6a. According to our analysis of the linewidths (Figs. 5d, 5e), the group of spots with a central velocity of −22.2 km/s can be identified with both the disk and outflow. The main, most numerous groups have central velocities of −15, −8.1, and −1.7 km/s, which are fairly close to the molecular cloud velocity, and we can reasonably link these to the disk. We can adopt for them the standard model of an expanding envelope, associated with the accretion disk of the source. The mean velocity of the groups at −15 and −1.7 km/s, which is equal to 6.6 km/s in magnitude, can be adopted as the expansion velocity of the envelope; this is a typical value.

The absence of an HII region demonstrates that the source is fairly young. Strong turbulent motions of gas can have a strong effect on the conditions in the medium. Turbulence can impede the formation of an HII region or slow its development [13].

Since no interferometric measurements were carried out for this source, especially during its period of very high activity, careful analyses of the variability of individual emission features provide our only tool for refining models of the source. The complexity in this consists in the very strong variability of the emission, which makes it very difficult, and sometimes impossible, to observe the full evolution of components using usual methods. Analyses based on correlations and anticorrelations of large numbers of components are also required. Such analyses will also enable us to obtain the main parameters of the turbulent gas motions, which is also of great interest.

4. RESULTS

Let us summarize the main results of our 14-year monitoring of the water maser in IRAS 21078+5211.

(1) We have presented a catalog of H_2O maser spectra in the 1.35-cm line toward the infrared source IRAS 21078+5211 for April 1992 to March 2006 (Fig. 1), with a mean interval between observational sessions of two months. The spectral resolution in radial velocity was 0.101 km/s, and increasing to 0.0808 km/s starting from the end of 2005.

(2) H_2O maser emission was observed in the V_{LSR} interval from −43 to 12 km/s, and was divided into three segments: a central one (from − 21 to 2.5 km/s) and two lateral ones (from −43 to −21 km/s and from 2.5 to 12 km/s). The central velocity of the H_2O spectrum when the master activity was highest (2002–2006) is about −7.5 km/s, which differs from the CO cloud velocity by only ≈ 1–2 km/s.

(3) Based on the radial-velocity variations and the tendency for the linewidth to increase with increasing flux, we conclude that the medium is strongly fragmented, and that there is a small-scale turbulent outflow of gas in the H_2O maser-emission region. This outflow could considerably impede the development of HII regions.

(4) The asymmetric distribution of the components in V_{LSR}, difference in the average linewidths for the central and lateral clusters of components, and fairly high radial velocities of the lateral components relative to the velocity of the molecular cloud (especially in periods of high activity of the protostar) suggest that the maser spots belong to different structures in the source: a disk and bipolar outflow.

(5) For the main groups of H_2O maser features, we propose a model with an envelope expanding at a velocity of about 6.6 km/s, which hosts these groups of maser spots.

ACKNOWLEDGMENTS

The RT-22 radio telescope is supported by the Ministry of Education and Science of the Russian Federation (facility registration number 01-10). This work was supported by the Russian Foundation for Basic Research (project code 06-02-16806-a). The authors are grateful to the staff of the Pushchino Radio Astronomy Observatory for their substantial help with the observations.

REFERENCES

1. F. Palla, R. Cesaroni, G. Comoretto, and M. Felli, Astron. Astrophys. **246**, 249 (1991).
2. J. G. A. Wouterloot, J. Brand, and K. Fiegle, Astron. Astrophys., Suppl. Ser. **98**, 589 (1993).
3. T. Jenness, P. F. Scott, and R. Padman, Mon. Not. R. Astron. Soc. **276**, 1024 (1995).
4. T. M. Dame and P. Thaddeus, Astrophys. J. **297**, 751 (1985).
5. J. P. Bernard, K. Dobashi, and M. Momose, Astron. Astrophys. **350**, 197 (1999).
6. M. Szymczak, G. Hrynek, and A. J. Kus, Astron. Astrophys., Suppl. Ser. **143**, 269 (2000).
7. B. A. Wilking, L. G. Mundy, J. H. Blackwell, and J. E. Howe, Astrophys. J. **345**, 257 (1989).
8. M. P. Miralles, L. F. Rodríguez, and E. Scalise, Astrophys. J., Suppl. Ser. **92**, 173 (1994).
9. J. M. Torrelles, N. A. Patel, G. Anglada, J. F. Gómez, et al., Astrophys. J. **598**, L115 (2003).
10. C. Codella, M. Felli, and V. Natale, Astron. Astrophys. **311**, 971 (1996).
11. E. E. Lekht, Astron. Zh. **72**, 532 (1995) [Astron. Rep. **72**, 472 (1995)].
12. E. E. Lekht, N. A. Silant'ev, V. V. Krasnov, and V. A. Munitsyn, Astron. Zh. **83**, 716 (2006) [Astron. Rep. **50**, 638 (2006)].
13. T. Xie, L. G. Mundy, S. N. Vogel, and P. Hofner, Astrophys. J. **473**, L131 (1996).

Translated by G. Rudnitskii